# A thermocouple-based remote temperature controller of an electrically-floated sample for plasma CVD of nanocarbons with bias voltage

Toshihiro Shimada[1,2], Takuya Miura[1], Wei Xie[1], Takashi Yanase[1,3], Taro Nagahama[1]

[1] Division of Applied Chemistry, Faculty of Engineering, Hokkaido University, Japan
Kita 13 Nishi 8, Kita-ku, Sapporo 060-8628, Japan

[2] CREST, Japan Science and Technology Agency, Chiyoda-ku, Tokyo 102-0076, Japan

[3] Frontier Chemistry Center, Hokkaido University, Kita-ku, Sapporo, 060-8628, Japan

Abstract

We report an accurate and easy-to operate instrument for the temperature control of an electrically-floated sample using a thermocouple in direct contact with it. The signal was transmitted via 2.45 GHz WiFi. We measured and analyzed the discrepancy between the thermocouple and a radiation thermometer for the plasma CVD of carbon nanomaterials under sample bias. A successful protection method from abnormal discharge in the plasma is also provided.

Key words: temperature measurement, plasma CVD, carbon nanomaterial, emissivity, pyrometer, thermocouple

Corresponding Author: Toshihiro SHIMADA

e-mail: shimadat@eng.hokudai.ac.jp

## 1. Introduction

Extension of electrochemical concepts to plasma processes are now gathering considerable attention from both the plasma community and electrochemistry community[1-10]. The distinct feature of plasma electrochemistry is its high energy and high temperature processes in combination with gas-surface interactions, as well as wide potential windows that the gaseous environment allows. From this point of view, the plasma CVD processes of carbon materials, such as bias enhanced nucleation of diamond thin films[11] ,aligned carbon nanotube forests[12] and their chirality control[13], are involved with a kind of electrochemical process in plasma because they are highly dependent on the bias voltage applied between the substrate and the chamber wall. In order to control the process, it is necessary to precisely measure the sample temperature, as already mentioned in the literature[2]. The temperature of the sample at high potential (>100 V) from the electrical ground level is usually monitored by an infrared thermometer or a pyrometer. However, there is a troublesome parameter, *i.e.* , the emissivity, during operation of the pyrometer. The emissivity is the ratio of the actual radiation from the sample surface at a certain wavelength to that from the blackbody at the same temperature. It is strongly dependent on the composition and morphology of the surface, and thus the value has to be calibrated when a different material is used[14,15]. The difficulty arises when the surface composition and morphology are changing in real time as in the plasma CVD process. On the other hand, if the temperature is not very high (<1500 $^{o}$C), contact measurement by a thermocouple can be a solution to this difficulty. It is thus highly required to develop a measurement scheme using a thermocouple with an electrically-floated sample. Due to the recent advancement of low power microcontrollers and WiFi technology, it is now

possible to do this, without a cumbersome optical cable connection[16] that has been the only recent solution.

Another severe problem during the high voltage experiment in the plasma environment is abnormal discharge events. They produce an intolerable voltage difference between the inputs of the thermocouple signal amplifier and high voltage and current to the heater power supply. We have tried various protection circuits and found a reliable solution.

In this paper, we describe the measurement and protection circuits for the temperature measurement and control of an electrically-floated sample using a thermocouple during the plasma CVD of carbon nanomaterials. We analyzed the difference between the readings of the thermocouple and pyrometer, and demonstrated the bias effect on the formation of carbon nanomaterials.

## 2. Experimental setup

Figure 1 displays the experimental setup. Figure 1 (a) illustrates the complete vacuum system and Figure 1 (b) shows the sample assembly. The sample was insulated by ceramic insulators from the chamber. We used a ϕ 10 mm ultrahigh-vacuum-compatible cartridge heater (Heat Wave Labs Co., Ltd., #101126) because of its high attainable temperature (1200 $^{o}$C) and low power consumption for small samples. The surface of the heater is insulated from its power leads by ceramics. This feature enables the use of a simple power supply not floated from the electrical ground. The heater was supported from three directions with set screws and 0.1mm-thick Ta foil. The sample was a 6mm x 6mm Si wafer with catalyst nanoparticles. It was attached to the heater surface (made of molybdenum) with

clamps. A chromel-alumel (K-type) thermocouple of ϕ 0.1 mm diameter was clamped on the sample surface. Most part of the thermocouple lead was electrically shielded and only small portion for detecting the temperature is exposed to the plasma. The non-shielded portion was affected by the potential deviation in the plasma, but there was no problem because the measurement circuit was electrically floated. The stability of the measured temperature values assures the measurement was correctly performed (see the result below) .

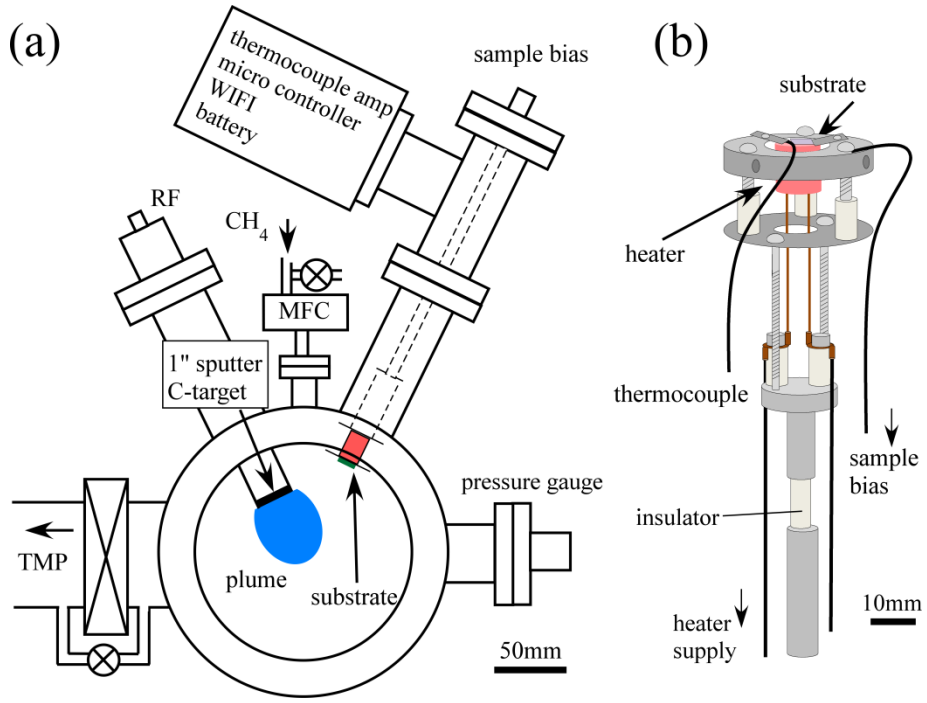


Figure 1: Experimental setup. (a) Overall schematics and (b) sample assembly.

Figure 2 shows the schematic circuit diagram of the temperature controller using an electrically-floated thermocouple. The electromotive force from the thermocouple is measured by a cold-junction-compensated K-thermocouple-to-digital converter (Maxim MAX6675) through a surge filter composed of coils, capacitors and diodes. The output

of the MAX6675 was transferred via an SPI bus to a microcontroller (Arduino Uno) with a ZigBee WiFi unit. The thermocouple converter and microcontroller were powered by a rechargeable lead-acid sealed battery (12V, 900mAh) and electrically insulated from the CVD chamber. The signals can be transmitted through a glass window, which enables the operation in a glove box, if necessary. Thermocouple readings were continuously transmitted to another ZigBee - microcontroller (Arduino Uno) - digital-to-analog (DA) converter (Microchip MCP4725) at one-second intervals. The 0-5V output of the DA converter was connected to the scalable temperature input

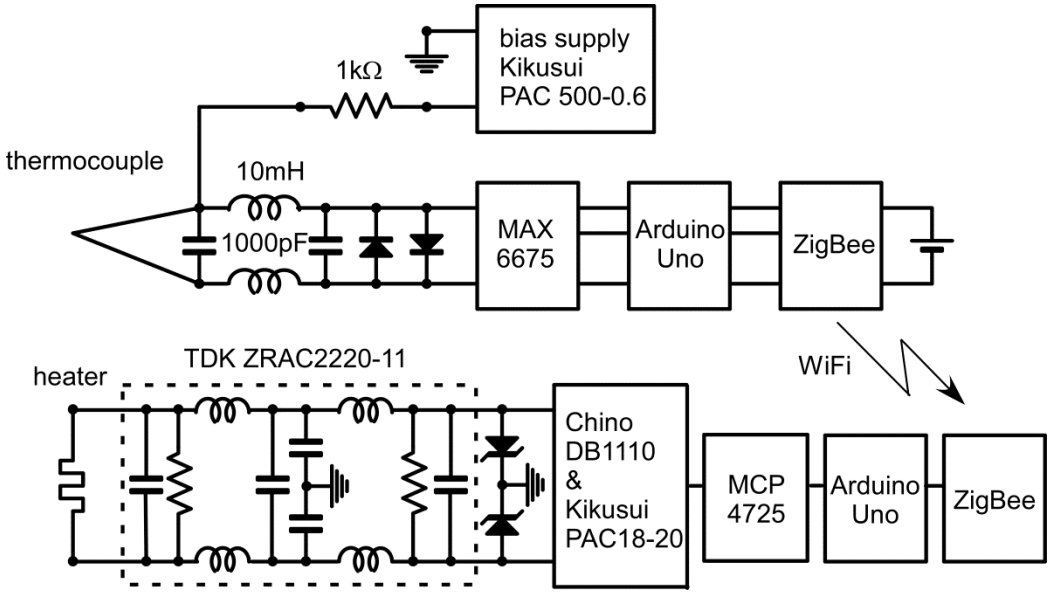


Figure 2: Measurement and control circuit diagram.

(scaled so that 0 - 5V corresponds to 0 - 1000°C) of a PID controller (Chino DB1110). The output of the PID controller was connected to a remote analog control input of a switching power supply (KIKUSUI PAC 18-20). The output of the switching power supply was connected to the sample heater through another protection circuit. The output protection circuit consisted of a line noise filter (TDK ZRAC2220-11) and two

Zener diodes that have a limiting voltage (20V) slightly higher than the output voltage of the switching power supply (18V). If a higher heater supply voltage is necessary, we found that gas discharge-type surge arresters (for example, Epcos A81-A230V) were also effective when used in place of the Zener diodes, although they were not needed in the experiments presented here.

The sample bias (0-500V) was supplied via a 1kΩ series resistor ($R$) from a switching power supply (KIKUSUI PAC 500-0.6). The current flowing in the sample ($I$) increased superlinearly with the bias voltage and was 10 mA at a 500V bias voltage. The $IR$ drop causes a maximum 10V voltage drop, which is low enough compared to the bias voltage. The series resistor effectively protected the bias supply from discharge.

The plasma for the CVD was generated by a RF magnetron sputtering gun equipped with a graphitic carbon plate target (Nilaco, Inc., 99.98%, 1-inch diameter) operated in $CH_4$ gas. The geometry of the substrate and the RF sputtering gun was carefully designed to avoid direct deposition from the sputtering gun[17,18]. Raman spectra were measured by Ranishaw inVia with a 532 nm laser. FE-SEM (JEOL JSM-6500FA) was used for the observation of the surface morphology of the grown materials.

## 3. Results and Discussion

### 3.1 Thermocouple versus Radiation Thermometer

Figure 3 shows the readouts of the thermocouple and the radiation thermometer (Japan Sensor FTZ6-R150, monitoring wavelength 1.95 - 2.5 μm) focusing on the sample surface during the plasma CVD of carbon at a floating voltage. The source gas was $CH_4$ (70 Pa, 20sccm) and the RF power consumed in the plasma was 20W. The sample bias was -400V. The substrate was a Si wafer spin-coated with Fe/Ni nanoparticles

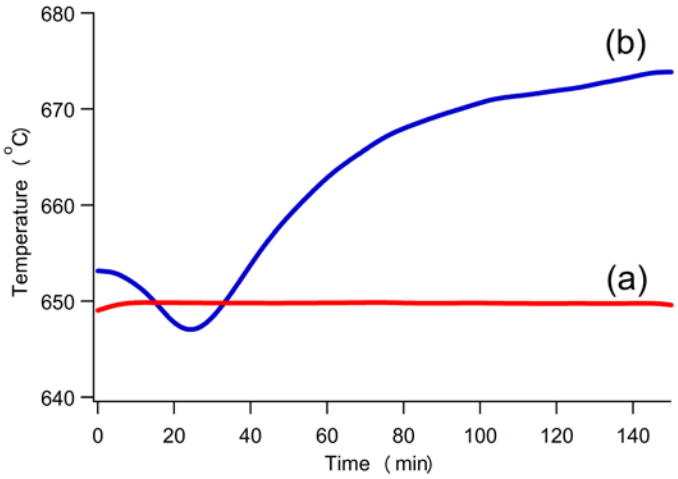


Figure 3: Temperature measured by (a) thermocouple ($T_T$) and (b) radiation pyrometer ($T_R$).

(Aldrich, diameter ~ 200 nm) dispersed in ethanol. The catalyst thoroughly covered the surface. The emissivity value for the radiation thermometer was adjusted to 0.32 when the sample reached 650 °C in a vacuum before the CVD in order to make it agree with the thermocouple read out ($T_T$). The sample temperature was controlled by the thermocouple reading and was stable within ± 1 °C. The radiation thermometer reading ($T_R$, Figure 3(b)) showed a significant deviation from $T_T$ (Figure 3(a)). After starting the growth (0 min), the $T_R$ increased by 3 °C (5min). It then started to decrease and reached -3 °C from $T_T$ (647 °C) at 20 min. Next, it started to increase and gradually saturated to the value of ~675 °C after 140 min from the start of the growth. The final $T_R$ value was 25 °C higher than $T_T$. This inaccuracy of $T_R$ is problematic for the plasma CVD process. The reason for this discrepancy will be discussed in the next section.

3.2 The mechanism for the discrepancy in the radiation thermometer readout

The temperature difference between the thermocouple and radiation thermometer is due to the change in the emissivity. In order to understand this mechanism, we stopped the CVD process at 20 min ($T_R = T_T - 2$ °C), 35 min ($T_R \simeq T_T$) and 150 min ($T_R = T_T + 25$ °C) and analyzed the films at each stage. The film morphologies are shown in Figure 4. Grains with 20-50 nm were observed on the catalyst powder (200nm diameter) in Figure 4(a) (20min). The grains grow as walls which are observed as curved lines in Figure 4(b) (35min), resembling so-called carbon nanowalls[19,20]. After the $T_R$ saturated, a terrace-like structure covered the surface as observed in Figure 4(c) (150 min).

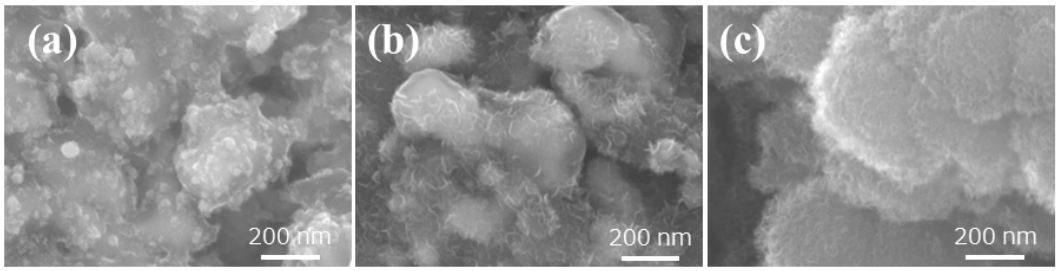


Figure 4: FE-SEM images of carbon deposited on catalyst grains. Growth time (a)20min, (b) 35min and (c) 150 min.

Figure 5 shows the Raman spectra of the stages in Figure 4. Since the Raman signal from the catalyst (665cm$^{-1}$, see Figure 6) was not observed in Figure 5, the surface was already covered by carbon. The D (~1350 cm$^{-1}$) and G (~1600 cm$^{-1}$) peaks from carbon were clearly observed. The ratio of peak areas between G/D slightly changes from (a) (G/D= 1.29) to (b) (G/D=1.73) but almost unchanged between (b) (G/D=1.73) and (c) (G/D=1.81). Therefore the change in the emissivity is not from the change in the chemical nature of the film.

From the apparent temperature rise when the film is thick, the emissivity of the deposited carbon is greater than that of the catalyst (Fe/Ni) surface. If this is assumed, the initial (< 5 min) rise of $T_R$ can also be explained because the carbon partly covers the surface of the catalyst. The decrease in the $T_R$ or temporary decrease in the emissivity between 5 min and 20 min cannot be explained by an ordinary coverage effect. We consider that it is due to the morphology during the initial stage of carbon nanowall formation. There are reports about the decrease of the emissivity caused by the destructive interference effect of microstructures [21-23].

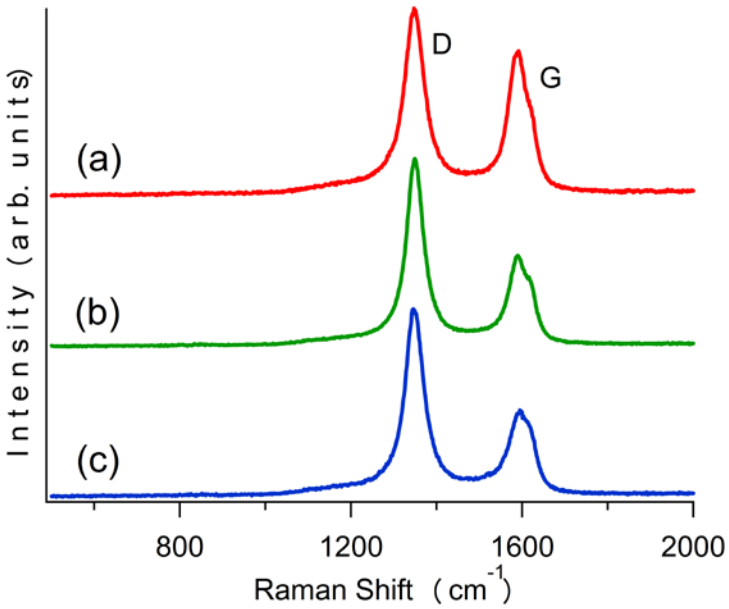


Figure 5: Raman spectra of carbon deposited on catalyst grains. Growth time (a)20min, (b) 35min and (c) 150 min.

3.3 Demonstration of the bias voltage effect: plasma CVD of nanocarbons with DC bias

We used the setup previously described to grow thin carbon films by plasma CVD. Figure 6 displays the Raman spectrum of the films grown at $T_f$=650 °C with the $CH_4$ pressure of 70 Pa, $CH_4$ flow rate 20sccm and RF power consumption of 20W. The bias

voltage to the sample

was changed between -100 V to -400 V. The growth time was 60 min. We can see that the radial breathing mode (RBM), that is, the signature of the existence of well-defined carbon nanotubes, can be observed only at the bias voltage of -200 V. We also notice that a Raman mode from the oxidized surface of Ni/Fe catalyst (630cm$^{-1}$, $Fe_3O_4$ and FeO)[24] was observed only from the samples prepared with -100 ~ -300V bias voltages. These results clearly show that the bias voltage is very important for controlling the chemical process involved in the plasma CVD growth of the carbon thin films.

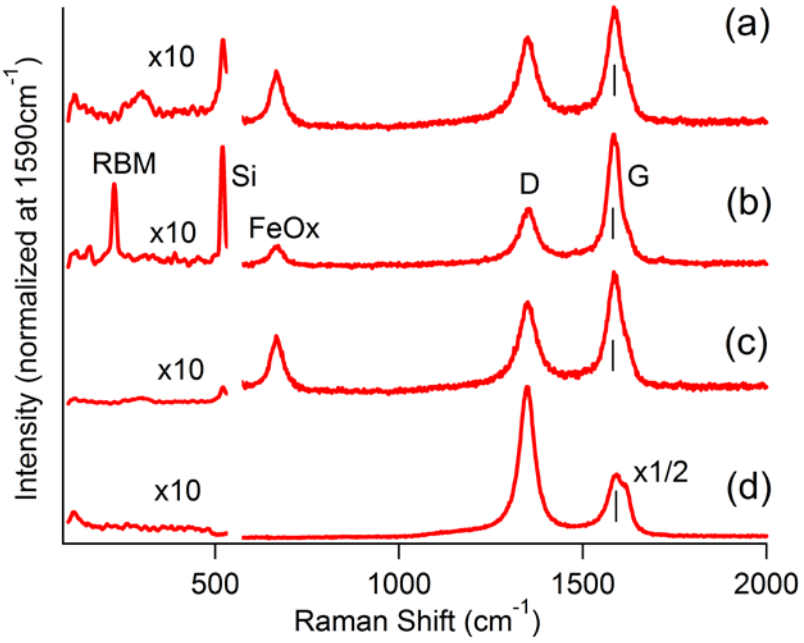


Figure 6: Raman spectra of carbon materials grown with different sample bias voltages. (a) -100V, (b) -200V, (c) -300V and (d) -400V.

3.4 Protection Circuits

Finally, we explain what happened without the protection circuits. We observed rare events of abnormal discharges in the plasma when high bias voltages were applied. When the abnormal discharge occurs, (i) the bias power supply tripped due to the surge

current, (ii) the thermocouple-to-digital converter was permanently damaged, and (iii) the heater power supply was permanently damaged. (i) usually does not cause a permanent damage, but the circuit breaker must be monitored to prevent the bias voltage stopping for a long time. This can be protected by the series resistor. (ii) is due to the voltage difference between the thermocouple elements caused by the surge, which ruins the amplifier. Since the thermocouple circuit is electrically floated, the surge current that flows into the circuit is negligible. The voltage difference can be protected by LC low pass filter and diodes. We found that (iii) is mainly due to the high reversing current to the heater power supply, which damages the copper plating in the printed circuits and the final stage transistors. This can be prevented by adding a line noise filter and surge arresters (gas discharge type or Zener diodes) that will dissipate the current pulse to the ground.

Ordinary electrochemical measurements use a reference electrode that monitors the potential of the electrolyte. In the low density plasma used in the present experiment, the potential is not uniform and precise monitoring of the potential distribution by various probes, including the reference electrodes[8], is also important. The protection circuit from discharge described here will be useful to avoid the damage of a battery -operated measurement circuit floated from the ground level.

## 4. Conclusion

We have developed an instrument for the accurate temperature control of an electrically-floated sample using a thermocouple directly in contact with it. A battery-operated microcontroller transmits the thermocouple reading to a PID heater controller via a 2.45GHz WiFi. We measured the difference between the thermocouple

reading and the infrared pyrometer during the plasma CVD of carbon materials and found that the difference can be +25 °C at 650 °C. We demonstrated the effect of applying a bias voltage to the sample during the growth of carbon nanotubes, in which only a -200V bias was successful. The protection method from the electrical discharge in the plasma was also provided.

Acknowledgment

This work was supported in part by a Grant-in-Aid for Scientific Research on Innovative Areas “Frontier Science of Interactions between Plasmas and Nano-Interfaces” (Grant No. 21110002) from the Ministry of Education, Culture, Sports, Science and Technology of Japan (MEXT). We would like to thank Professor T. Hasegawa (The University of Tokyo) for his valuable discussions and support through the JST-CREST program. The experimental work was conducted at Hokkaido University supported by the “Nanotechnology Platform” Program of MEXT.

References

1. D.J. Caruana, S.P. McCormack, Electrochem. Commun. 2, 816 (2000).

2. J.M. Goodings, J. Guo, A.N. Hayhurst, S.G. Tayker, Int. J. Mass. Spectr. 206, 137 (2001).

3. J.M. Goodings, J. Guo, J. G. Laframboise, Electrochem. Commun. 4, 363 (2002).

4. E. Hadzifejzovic, J.A..Sanchez Galiani, D.J. Caruana, Phys. Chem. Chem. Phys. 8, 2797 (2006).

S. A. Meiss, M. Rohnke, L. Kienle, S.Z. El Abedin, F. Endres, J. Janek, ChemPhysChem 8, 50 (2007).

5. E. Hadzifejzovic, J.Stankovic, S. Firth, P.F. McMillan, D.J. Caruana, Phys. Chem. Chem. Phys. 9, 5335 (2007).

M. Brettholle, O. Höfft, L. Klarhöfer, S. Mathes, W. Maus-Friedrichs, S. Z. El Abedin, S. Krischok, J. Janek, F. Endres, Phys.Chem.Chem.Phys. 12, 1750 (2010)

6. C.Richmonds, M. Witzke, B. Bartling, S.W. Lee,J. Wainright, C.C. Liu, R. M. Sankaran, J. Am. Chem. Soc. 133, 17582 (2011).

7. A. Elahi, T. Fowowe, D.J.Caruana, Angew. Chem. Int. Ed. 41, 6350 (2012).

8.T. Fowowe, E. Hadzifejzovic, J. Hu, J.S. Foord, D.J. Caruana, Adv. Mater. 24, 6305 (2012).

9. R. Akolkar, R.M. Sankaran, J. Vac. Sci. Technol. A31, 050811 (2013).

10. M. Bouchard, M. Letournaeau, C. Sarra-Bournet, M. Laprise-Pelletier, S. Turgeon, P. Chevallier, J. Kaueux, G. Laroche, M.A. Fortin, Langmuir, 31, 7633 (2015).

11. S. Yugo, T. Kanai, T. Kimura, T. Muto, Appl. Phys. Lett. 58, 1036 (1991).

12. G. F. Zhong, T. Iwasaki, J. Robertson, H. Kawarada, J. Phys. Chem. B 111, 1907 (2007).

13. Z. Ghorannevis, T. Kato, T. Kaneko, R. Hatakeyama, J. Am. Chem. Soc. 132, 9570 (2010).

14. H. Zhang, W. Xia, G. Wang, Y. Yang, and Y. Zou, J. Themal Spray Technol. 17, 263 (2008).

15. H. Madura and T. Piatkowski, Infrared Phys. Technol. 46, 185 (2004).

16. S. Ruan and O.H. Kapp, Rev. Sci. Instr. 66, 4313 (1995).

17. W. Xie, N. Muraya, T. Yanase, T. Nagahama, T. Shimada, Jpn. J. Appl. Phys. **53**, 010203 (2014).

18. W. Xie, A. Kawahito, T. Miura, T. Endo, Y. Wang, T. Yanase, T. Nagahama, Y. Otani,

T. Shimada, Chem. Lett. 44, 1205 (2015).

19. Y. Wu, P. Qiao, T. Chong, Z. Shen, Adv. Mater. 14, 64(2002).

20. M .Hiramatsu, M. Hori, Jpn. J. Appl. Phys. 45, 5522 (2006).

21. F. Marquier, K. Joulain, J.P. Mulet, R. Carminati, J.J. Greffe, Optics Commun. 237, 379 (2004).

22. T. Matsumoto, M. Tomita, Optics Express 18, A192 (2010).

23. G. Feng, Y. Li, Y. Wang, P. Li,J. Zhu, L. Zhao, Opt. Lett. 37, 299 (2012).

24. D. L. A. de Faria, S. Venaüncio Silva, M. T. de Oliveira, J. Raman Spectr. 28, 873 (1997).